From quarks to hadrons and back - spectral and bulk phenomena of strongly interacting matter

2015 J. Phys.: Conf. Ser. 640 012053

(http://iopscience.iop.org/1742-6596/640/1/012053)

Journal of Physics: Conference Series **640** (2015) 012053 doi:10.1088/1742-6596/640/1/012053

From quarks to hadrons and back - spectral and bulk phenomena of strongly interacting matter

Stefan Krieg
Budapest-Marseille-Wuppertal and Wuppertal-Budapest collaborations
Department of Physics, University of Wuppertal, Gaußstr. 20, D-42119, Germany
IAS, Jülich Supercomputing Centre, Forschungszentrum Jülich, Jülich, D-52425, Germany

Abstract. Recent results on the proton-neutron mass splitting, relevant for the stability of ordinary matter, and on the properties of matter in under extreme conditions as created by heavy ion experiments, obtained through numerical simulations of Lattice Quantum Chromo- and Electrodynamics are discussed.

1. Introduction

Computing, from first principles, the hadron masses to percent accuracy [1], is only possible through simulations of Lattice Quantum Chromodynamics (QCD). With the advent of the present class of Pflop Machines and novel simulation algorithms, we now can proceed to compute per-mil effects in the particle spectrum, i.e., the proton-neutron mass difference. This difference is due to a subtle cancellation of already small effects (due to the mass difference of the up- and down-quarks and the presence of electromagnetic interactions). In the first part of these proceedings, we report on a project [2, 3] to compute this and other mass differences using simulations of Lattice Quantum Chromo- and Electrodynamics and discuss the new simulation methods and the highly efficient code employed.

In the case of the proton and the neutron, quarks and gluons are confined to the hadron. If we, however, increase the temperature of the system sufficiently, both particles will 'melt' and quarks and gluons behave as free particles ('quark-gluon-plasma'). This transition is described by the Equation of State (EoS) of QCD [4]. In the second half of these proceedings, we discuss a full result for the EoS [5] *excluding* as well as an ongoing project (e.g. [6, 7]) aimed at calculating the EoS *including* the effects of a dynamical charm quark, which becomes relevant for temperatures larger than 300-400 MeV.

2. Mass splittings from simulations of Lattice Quantum Electro- and Chromodynamics

Lattice Quantum Chromodynamics (LQCD) has matured significantly over the last decade. By now, calculations of many properties of strongly interacting matter are available. Simpler quantities such as proton and neutron masses are routinely computed to percent precision in the continuum limit [1, 8, 9, 10]. Properties of nucleons computed on the lattice, such as the charge radius of the proton, agree with experiment (see, e.g., [11, 12, 13], for a recent review see [14]). In this particular case, however, the level of precision reached does not allow one to solve the

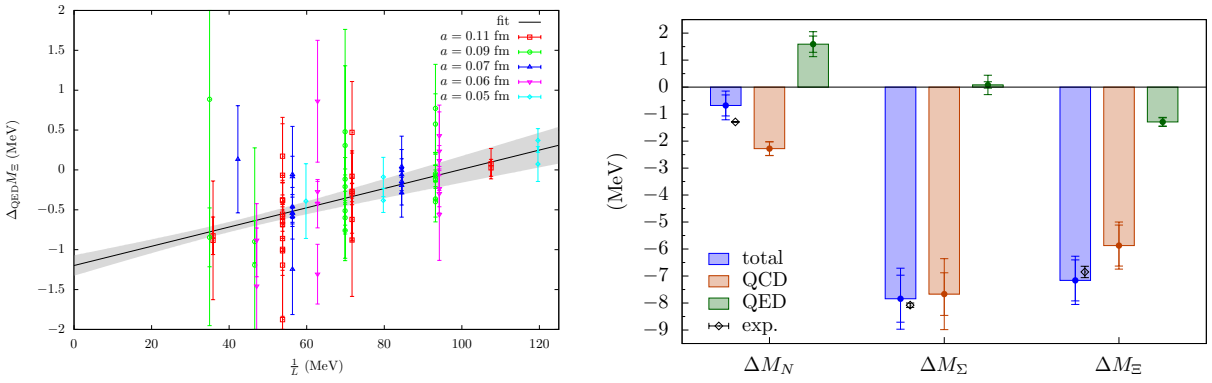

Figure 1. *Left:* Finite size effects due to QED. Shown is the dependence of the QED part of the Xi splitting on the inverse box size L. *Right:* Final result for the mass splittings. In this calculation [2], the achieved precision for the proton-neutron mass splitting (ΔM_N) excludes zero by slightly more than one sigma.

"proton radius puzzle" [15] for which better control of systematics, such as excited state effects, is required.

For hadron mass splittings, permill precision has been reached already [2, 3]. These calculations calculate splittings in hadron masses due to the violations of the (approximate) isospin symmetry in nature, i.e., due to mass and electromagnetic charge differences between the different quark flavors. In [2] these small effects were included by simulating lattice QCD+QED in the electro-quenched approximation, where the sea quarks were uncharged (and, as a matter of fact, up and down quarks were mass-degenerate). The most challenging problem faced by such calculations including electro-magnetic effects are finite-size effects. This is illustrated on the l.h.s. of Figure 1. The most significant caveat of this calculation is the fact that the signal is of the same order as the leading source of error due to the uncharged sea quarks.

This can only be remedied by a fully dynamical calculation, including dynamical QED and non-degenerate quark masses. Such a calculation was presented in [3]. For it to be successful, a range of issues had to be addressed. The hadron propagators suffer from unphysical contributions that are proportional to the quark charges e_q, the signal being of order e_q^2. In the case of the aforementioned quenched QED calculation with uncharged sea quarks, one could average propagators with negative and positive charges, thereby eliminating the $O(e_q)$ contributions to the results. This is, however, not possible in an unquenched simulation. The approach taken was, therefore, to simulate at larger than physical charges, where the noise is much smaller, and to use a set of ensembles with uncharged quarks to interpolate to the physical point. It also turns out that the previously used method to subtract problematic zero modes of QED (which is permissible since these are of zero measure in the continuum) violated reflection positivity. As a consequence there are no mass plateaus and results depend on the ratio of the temporal over spatial box size (T/L). By subtracting more modes (also of zero measure), however, this problem could be solved. As mentioned above, finite size effects are large when QED is included in the calculation. For the target precision aimed at in this project, since the finite size deviations dominate the signal, the first to terms of the $1/L$ expansion were calculated analytically and shown to be universal. The non-universal coefficient of the $1/L^3$ term (which depends, among others, on the charge radius) was then fitted. In order to be certain that this setup is correct, dedicated pure QED simulations were performed to check the finite volume correction terms. A new "fourier accelerated" HMC was used to update the QED fields, since the generic method suffered from extremely long autocorrelations. The propagator calculations were sped up using

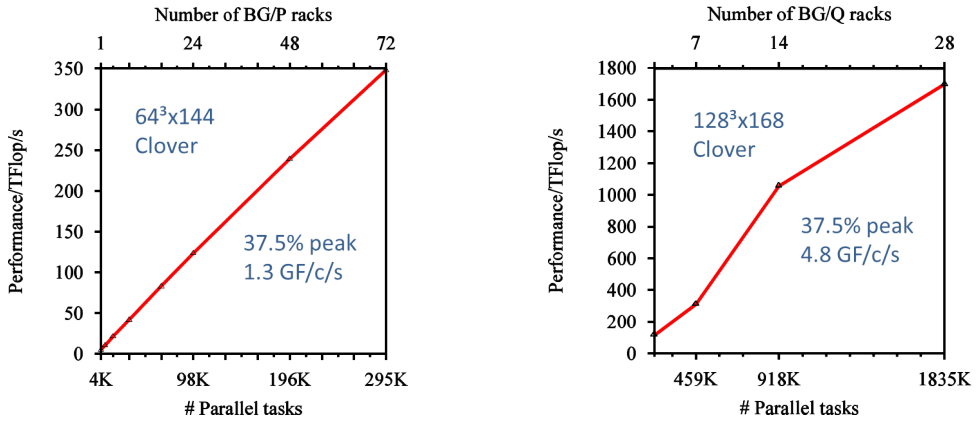

Figure 2. *Left:* Perfect strong scaling as seen on the (now obsolete) Blue Gene/P. Up to 300,000 parallel threads could be run at a sustained performance of about 350 TFlop/s. *Right:* Strong scaling on the Blue Gene/Q. On this architecture and the lattice size chosen for the strong scaling analysis, a sweet spot at about 1,000,000 parallel threads can be seen. At 1,800,000 parallel threads we achieve, for this particular lattice volume, a sustained performance of about 1.7 PFlop/s.

a new multilevel-method [16, 17] combined with "all mode averaging" [18]. Finally, the analysis combined a Kolmogorov-Smirnov analysis for the fit intervals with the histogram method of [1] and was crosschecked independently. The final results [3] now exclude zero for the proton-neutron mass splitting on the five sigma level and make predictions for other mass splittings that have not yet been measured or where the experimental uncertainties are significantly larger.

3. Performance

Our simulation software has been ported to a range of different architectures, such as clusters (e.g., "Juropa" at JSC, Jülich) or highly scalable architectures such as Blue Gene/Q, Cray XE6, or Cray XC40 (e.g., "Hermit" and "Hornet" at HLRS, Stuttgart or "Juqueen" at JSC, Jülich). In Figure 2 we show the performance obtained on the Blue Gene/Q architecture. Our code scales well up to 1.8 million hardware threads or the full 28 Racks of "Juqueen". We have hand-tuned both the parallel and serial parts of the code. The performance of the multi-shift CG used in the RHMC [19] algorithm achives a sustained performance of 3.2 GFlop/core/s (CG is more efficient, BiCGstab similar) and the considerably more complicated multi-level solver [16, 17] reaches 2.0 GFlop/core/s (but converges, compared to e/o preconditioned BiCGstab, orders of magnitude faster [16]).

4. Full result for the $N_f = 2 + 1$ equation of state

The rapid transition from the quark-gluon-plasma 'phase'[1] to the hadronic phase in the early universe and the QCD phase diagram are subjects of intense study in present heavy-ion experiments (LHC@CERN, RHIC@BNL, and the upcoming FAIR@GSI). This transition can be studied in a systematic way in Lattice QCD (for recent reviews see, e.g., [21, 22, 23, 10]). The equation of state (EoS) of QCD, (i.e, the pressure p, energy density ϵ, trace anomaly $I = \epsilon - 3p$, entropy $s = (\epsilon + p)/T$, and the speed of sound $c_s^2 = dp/d\epsilon$ as functions of the temperature) has been determined by several lattice groups, however, a full result has only recently become

[1] Since this transition is a cross-over [20], this use of the term 'phase' is somewhat abusive, and indicates only the dominant degrees of freedom.

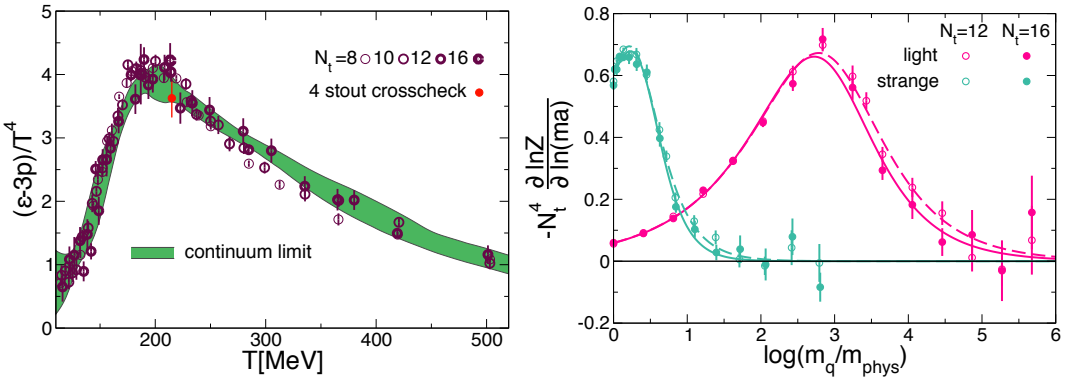

Figure 3. *Left:* The trace anomaly as a function of the temperature. The continuum extrapolated result with total errors is given by the shaded band. Also shown is a cross-check point computed in the continuum limit with our new and improved lattice action at $T = 214$ MeV, indicated by a smaller filled red point, which serves as a crosscheck on the peak's height. *Right:* Setting the overall scale of the pressure: integration from the infinitely large mass region down to the physical point using a range of dedicated ensembles and time extents up to $N_t = 16$; the sum of the areas under the curves gives p/T^4.

available: reference [4] constitutes a full result at three characteristic temperatures, which we have now extended to the full temperature range and made available electronically [5] .

Our calculation is based on a tree-level Symanzik improved gauge action with 2-step stout-link improved staggered fermions. The precise definition of the action can be found in ref. [24], its advantageous scaling properties are studied in ref. [25, 26, 27].

We include two different scale setting procedures in our 'histogram' method [1] used to estimate systematical errors, along with a range of other fit methods, each of which is an in principle completely valid approach. We then calculated the goodness of fit Q and weights based on the Akaike information criterion AICc [28, 29] and looked at the unweighted or weighted (based on Q or AICc) distribution of the results. The median is the central value, whereas the central region containing 68% of all the possible methods gives an estimate on the systematic uncertainties. This procedure provides very conservative errors. Here, we used four basic types of continuum extrapolation methods, two continuum extrapolation ranges, seven ways to determine the subtraction term at T=0, and the aforementioned two scale procedures. Finally, we included eight options to determine the final trace anomaly by choosing among various spline functions, giving altogether 4·2·7·2·8=896 methods. Note that using either an AICc or Q based distribution changed the result only by a fraction of the systematic uncertainty. Furthermore, the unweighted distribution always delivered consistent results within systematical errors.

The continuum extrapolated trace anomaly is shown in Figure 3.

5. Update on the $N_f = 2 + 1 + 1$ Equation of State

So far, the equation of state is known only in 2+1 flavor QCD. The contribution from the sea charm quarks most likely matter at least for $T > 300 - 400$ MeV (for an illustration, see Figure 4).

The $N_f = 2+1$ lattice results of the previous section agree with the HRG at low temperatures and are correct for small to medium temperatures, and, as is shown in Figure 4, at temperatures of about 1 GeV perturbative results become sufficiently precise. Therefore, we need to calculate the EoS with a dynamical charm only for the remaining temperatures in the region of

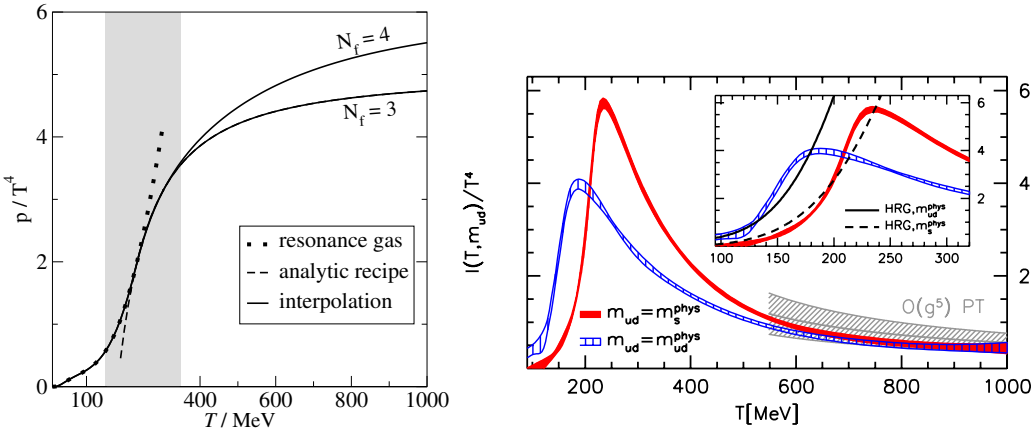

Figure 4. *Left:* Laine and Schroeder's perturbative estimate of the effect of the charm in the QCD equation of state [30]. *Right:* Wuppertal-Budapest [4] and perturbative (up to $O(g^5)$) results for the equation of state.

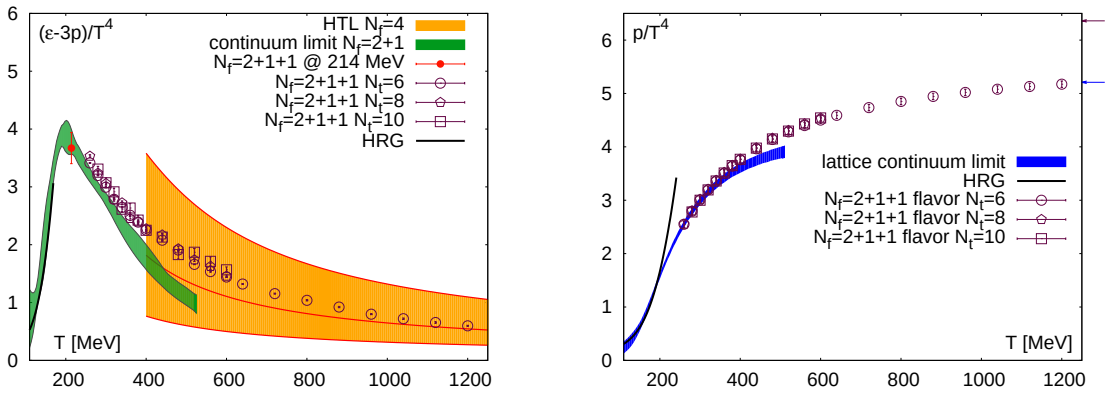

Figure 5. *Left:* Preliminary results for the charmed EoS. For comparison, we show the HRG result, the $N_f = 2+1$ band, and, at high Temperatures, the HTL result [31], where the central line marks the HTL expectation for the EoS with the band resulting from (large) variations of the renormalization scale. *Right:* Preliminary result for the pressure, errors indicate the Stefan-Boltzmann value. All errors are statistical only.

approximately 300 MeV $< T <$ 1000 MeV.

We are using a new lattice action for these calculations. More precisely, where our $N_f = 2+1$ calculation used an action with 2 levels of stout gauge link averaging in the coupling of the fermions to the gauge fields, we increased this to 4 levels with a smearing parameter of $\rho = 0.125$ (for further details see [5]). The crosscheck point shown in Figure 3 was computed using this new action. Since it perfectly agrees with the $N_f = 2+1$ results, even though it was computed using a dynamical charm, we can be certain that at temperatures at and below $T = 214$ MeV, we can rely on the $N_f = 2+1$ results.

Our preliminary results are shown in Figure 5, all errors are statistical only. Our results span a region of temperatures from $T = 214$ MeV up to $T = 1.2$ GeV. At the low end we make contact to the $N_f = 2+1$ equation of state, and at large temperatures to the HTL result. We thus cover the full region of temperatures, from low temperatures, where the HRG gives reliable

results, to high temperatures, where we make contact with perturbation theory. Our present set of data points will be extended to $N_t = 12$, in order to allow for a controlled continuum extrapolation.

6. Conclusions

The precision of Lattice QCD results at finite temperature has increased significantly over the last years. We discussed how permill level precision could be achieved for the particle spectrum of QCD, presented a full result (all sources of uncertainties controlled) for the $N_f = 2+1$ EoS [5], and shown how to include a dynamical charm quark for the $N_f = 2 + 1 + 1$ EoS and presented preliminary results.

Acknowledgments

Computations were performed on JUQUEEN at Forschungszentrum Jülich, HERMIT at HLRS, Stuttgart, and on the QPACE machine and on GPU clusters [32] at University of Wuppertal. We acknowledge PRACE for awarding us resources on JUQUEEN at Forschungszentrum Jülich. This work was partially supported by the DFG Grant SFB/TRR 55 and ERC no. 208740.

References

[1] Durr S, Fodor Z, Frison J, Hoelbling C, Hoffmann R *et al.* 2008 *Science* **322** 1224–1227 (*Preprint* 0906.3599)
[2] Borsanyi S, Drr S, Fodor Z, Frison J, Hoelbling C *et al.* 2013 *Phys.Rev.Lett.* **111** 252001 (*Preprint* 1306.2287)
[3] Borsanyi S, Durr S, Fodor Z, Hoelbling C, Katz S *et al.* 2014 (*Preprint* 1406.4088)
[4] Borsanyi S, Endrodi G, Fodor Z, Jakovac A, Katz S D *et al.* 2010 *JHEP* **1011** 077 (*Preprint* 1007.2580)
[5] Borsanyi S, Fodor Z, Hoelbling C, Katz S D, Krieg S *et al.* 2014 *Phys.Lett.* **B730** 99–104 (*Preprint* 1309.5258)
[6] Ratti C, Borsanyi S, Endrodi G, Fodor Z, Katz S D *et al.* 2013 *Nucl.Phys.* **A904-905** 869c–872c
[7] Borsanyi S, Fodor Z, Hoelbling C, Katz S D, Krieg S *et al.* 2014 (*Preprint* 1410.7917)
[8] Fodor Z and Hoelbling C 2012 *Rev.Mod.Phys.* **84** 449 (*Preprint* 1203.4789)
[9] Kronfeld A S 2012 *Ann.Rev.Nucl.Part.Sci.* **62** 265–284 (*Preprint* 1203.1204)
[10] Hoelbling C 2014 (*Preprint* 1410.3403)
[11] Green J, Engelhardt M, Krieg S, Negele J, Pochinsky A *et al.* 2014 *Phys.Lett.* **B734** 290–295 (*Preprint* 1209.1687)
[12] Green J, Negele J, Pochinsky A, Syritsyn S, Engelhardt M *et al.* 2012 *Phys.Rev.* **D86** 114509 (*Preprint* 1206.4527)
[13] Green J, Negele J, Pochinsky A, Syritsyn S, Engelhardt M *et al.* 2014 *Phys.Rev.* **D90** 074507 (*Preprint* 1404.4029)
[14] Constantinou M 2014 *PoS* **LATTICE2014** 001 (*Preprint* 1411.0078)
[15] Pohl R, Antognini A, Nez F, Amaro F D, Biraben F *et al.* 2010 *Nature* **466** 213–216
[16] Frommer A, Kahl K, Krieg S, Leder B and Rottmann M 2013 (*Preprint* 1307.6101)
[17] Frommer A, Kahl K, Krieg S, Leder B and Rottmann M 2014 *SIAM J. Sci. Comput.,* **36** A1581–A1608 (*Preprint* 1303.1377)
[18] Blum T, Izubuchi T and Shintani E 2013 *Phys.Rev.* **D88** 094503 (*Preprint* 1208.4349)
[19] Clark M and Kennedy A 2007 *Phys.Rev.Lett.* **98** 051601 (*Preprint* hep-lat/0608015)
[20] Aoki Y, Endrodi G, Fodor Z, Katz S and Szabo K 2006 *Nature* **443** 675–678 (*Preprint* hep-lat/0611014)
[21] Fodor Z and Katz S 2009 (*Preprint* 0908.3341)
[22] Philipsen O 2013 *Prog.Part.Nucl.Phys.* **70** 55–107 (*Preprint* 1207.5999)
[23] Petreczky P 2012 *PoS* **ConfinementX** 028 (*Preprint* 1301.6188)
[24] Aoki Y, Fodor Z, Katz S and Szabo K 2006 *JHEP* **0601** 089 (*Preprint* hep-lat/0510084)
[25] Aoki Y, Fodor Z, Katz S and Szabo K 2006 *Phys.Lett.* **B643** 46–54 (*Preprint* hep-lat/0609068)
[26] Aoki Y, Borsanyi S, Durr S, Fodor Z, Katz S D *et al.* 2009 *JHEP* **0906** 088 (*Preprint* 0903.4155)
[27] Borsanyi S *et al.* 2010 *JHEP* **1009** 073 (*Preprint* 1005.3508)
[28] Akaike H 1974 *IEEE Transactions on Automatic Control* **19** 716–723
[29] Hurvich C and Tsai C L 1989 *Biometrica* **76** 297–307
[30] Laine M and Schroder Y 2006 *Phys.Rev.* **D73** 085009 (*Preprint* hep-ph/0603048)
[31] Andersen J O, Leganger L E, Strickland M and Su N 2011 *JHEP* **1108** 053 (*Preprint* 1103.2528)
[32] Egri G I, Fodor Z, Hoelbling C, Katz S D, Nogradi D *et al.* 2007 *Comput.Phys.Commun.* **177** 631–639 (*Preprint* hep-lat/0611022)